

s AND t UNITARITY SCREENINGS  
AS FUNDAMENTAL INGREDIENTS  
IN SOFT SCATTERING

Uri Maor

Collaboration with E. Gotsman and E. Levin

*Raymond and Beverly Sackler Faculty of Exact Science*

*Tel Aviv University, Tel Aviv, 69978, Israel*

**EDS 2013, SEPTEMBER 9-13, LAPLAND-FINLAND**

## INTRODUCTION

s channel Unitarity screening considerations date back to the ISR epoch, where they provided a simple way out of seemingly paradoxical traps.

1) Given that non screened  $\sigma_{tot}$  grows with energy,  $\sigma_{el}$  grows faster (optical theorem). With no screening,  $\sigma_{el}$  will, eventually, be larger than  $\sigma_{tot}$ .

2) Even though elastic and diffractive scatterings are dynamically similar, the energy dependence of diffractive cross sections is significantly more moderate.

3) The elastic amplitude is central in impact parameter  $b$ , peaking at  $b=0$ .

The diffractive amplitudes are peripheral, peaking at large  $b$ , which gets larger with energy.

40 years latter, estimates of soft scatterings channels at the TeV-scale require a unified analysis of elastic and diffractive scatterings, incorporating the Good-Walker mechanism and s and t unitarity screenings.

## S-CHANNEL UNITARITY

The simplest s-channel unitarity bound on  $a_{el}(s, b)$  is obtained from a diagonal re-scattering matrix, where repeated elastic re-scatterings secure s-channel unitarity,  $2Ima_{el}(s, b) = |a_{el}(s, b)|^2 + G^{in}(s, b)$ .

i.e. At a given  $(s, b)$ ,  $\sigma_{tot} = \sigma_{el} + \sigma_{inel}$ . Its general solution is:

$$a_{el}(s, b) = i \left(1 - e^{-\Omega(s, b)/2}\right), \quad G^{in}(s, b) = 1 - e^{-\Omega(s, b)}. \quad \Omega \text{ is arbitrary.}$$

The output s-unitarity bound is  $|a_{el}(s, b)| \leq 2$ , leading to very large total and elastic LHC cross sections, which are not supported by LHC recent data.

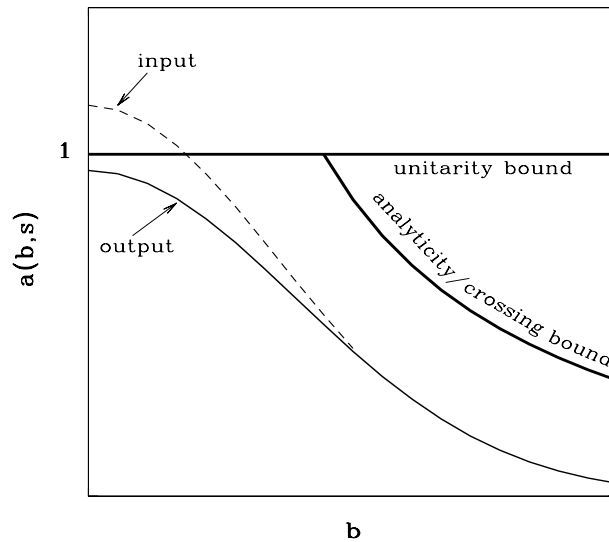
In a Glauber/Gribov eikonal approximation, the input opacity  $\Omega(s, b)$  is real.

It equals to the imaginary part of the input Born term, a Pomeron exchange in our context. The output  $a_{el}(s, b)$  is imaginary.

The consequent bound is  $|a_{el}(s, b)| \leq 1$ , which is the black disc bound.

In a single channel eikonal model, the screened cross sections are:

$$\sigma_{tot} = 2 \int d^2b \left(1 - e^{-\Omega(s, b)/2}\right), \quad \sigma_{el} = \int d^2b \left(1 - e^{-\Omega(s, b)/2}\right)^2, \quad \sigma_{inel} = \int d^2b \left(1 - e^{-\Omega(s, b)}\right).$$



The figure shows the s-channel black bound, and the **analyticity/crossing bound** implied by the  $\ln^2(s)$  expanding amplitude radius. The consequent **Froissart-Martin bound** is:  $\sigma_{tot} \leq C \ln^2(s/s_0)$ ,  $s_0 = 1\text{GeV}^2$ ,  $C \propto 1/2m_\pi^2 \simeq 30\text{mb}$ . **C** is far too large to be relevant at the **TeV-scale**.

**s-unitarity** implies:  $\sigma_{el} \leq \frac{1}{2}\sigma_{tot}$  and  $\sigma_{inel} \geq \frac{1}{2}\sigma_{tot}$ . **At saturation**,  $\sigma_{el} = \sigma_{inel} = \frac{1}{2}\sigma_{tot}$ .

Introducing diffraction, significantly changes the features of s-unitarity.

**However, the saturation signatures remain valid.**

## GOOD-WALKER DECOMPOSITION

Consider a system of two orthonormal states, a hadron  $\Psi_h$  and a diffractive state  $\Psi_D$ .  $\Psi_D$  replaces the continuous diffractive Fock states. Good-Walker (GW) noted that  $\Psi_h$  and  $\Psi_D$  do not diagonalize the 2x2 interaction matrix  $\mathbf{T}$ . Let  $\Psi_1$  and  $\Psi_2$  be eigen states of  $\mathbf{T}$ .

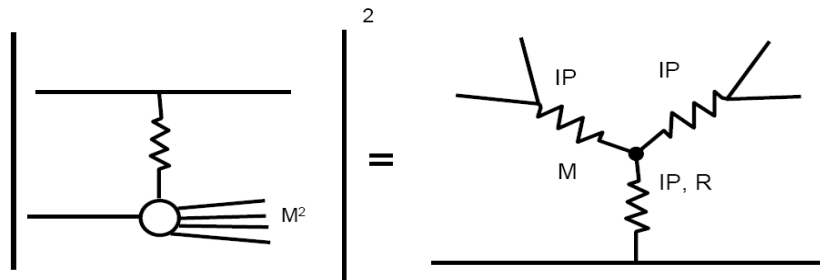
$$\Psi_h = \alpha\Psi_1 + \beta\Psi_2, \quad \Psi_D = -\beta\Psi_1 + \alpha\Psi_2, \quad \alpha^2 + \beta^2 = 1.$$

The eigen states initiate 4  $A_{i,k}$  elastic GW amplitudes ( $\psi_i + \psi_k \rightarrow \psi_i + \psi_k$ ).  $i,k=1,2$ . For initial  $p(\vec{p}) - p$  we have  $A_{1,2} = A_{2,1}$ . I shall follow the GLM definition, in which the mass distribution of  $\Psi_D$  is not defined and requires a specification. The elastic, SD and DD amplitudes in a 2 channel screened GW model are:

$$\begin{aligned} a_{el}(s, b) &= i\{\alpha^4 A_{1,1} + 2\alpha^2\beta^2 A_{1,2} + \beta^4 A_{2,2}\}, \\ a_{sd}(s, b) &= i\alpha\beta\{-\alpha^2 A_{1,1} + (\alpha^2 - \beta^2)A_{1,2} + \beta^2 A_{2,2}\}, \\ a_{dd}(s, b) &= i\alpha^2\beta^2\{A_{1,1} - 2A_{1,2} + A_{2,2}\}, \\ A_{i,k}(s, b) &= \left(1 - e^{\frac{1}{2}\Omega_{i,k}(s,b)}\right) \leq 1. \end{aligned}$$

Introducing t-channel screening results in a distinction between GW and non GW diffraction. In the GW sector:

- **We obtain the Pumplin bound:**  $\sigma_{el} + \sigma_{diff}^{GW} \leq \frac{1}{2}\sigma_{tot}$ .  
 $\sigma_{diff}^{GW}$  is the sum of the GW soft diffractive cross sections.
- **Below saturation,**  $\sigma_{el} \leq \frac{1}{2}\sigma_{tot} - \sigma_{diff}^{GW}$  **and**  $\sigma_{inel} \geq \frac{1}{2}\sigma_{tot} + \sigma_{diff}^{GW}$ .
- $a_{el}(s, b) = 1$ , **when and only when,**  $A_{1,1}(s, b) = A_{1,2}(s, b) = A_{2,2}(s, b) = 1$ .
- When  $a_{el}(s, b) = 1$ , all diffractive amplitudes at the same (s,b) vanish.
- **GW saturation signatures are valid also in the non GW sector.**
- **The saturation signature,**  $\sigma_{el} = \sigma_{inel} = \frac{1}{2}\sigma_{tot}$ , **in a multi channel calculation is coupled to**  $\sigma_{diff} = 0$ . **Consequently, prior to saturation the diffractive cross sections stop growing and start to decrease with energy.**  
**This is a clear signature preceding saturation.**



## CROSSED CHANNELED UNITARITY

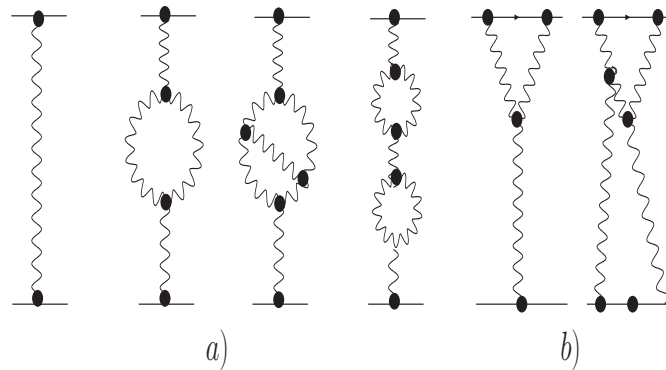
Translating the concepts presented into a viable phenomenology requires a specification of  $\Omega(s, b)$ , for which Regge Pomeron ( $IP$ ) theory is a powerful tool.

Mueller(1971) applied 3 body unitarity to equate the cross section of

$a + b \rightarrow M_{sd}^2 + b$  to the triple Regge diagram  $a + b + \bar{b} \rightarrow a + b + \bar{b}$ , with a leading  $3IP$  vertex term.

The  $3IP$  approximation is valid when  $\frac{m_p^2}{M_{sd}^2} \ll 1$  and  $\frac{M_{sd}^2}{s} \ll 1$ .

The leading energy/mass dependences are  $\frac{d\sigma^{3IP}}{dt dM_{sd}^2} \propto s^{2\Delta_{IP}} \left(\frac{1}{M_{sd}^2}\right)^{1+\Delta_{IP}}$ .



Mueller's  $3IP$  approximation for non GW diffraction is the lowest order of t-channel multi  $IP$  interactions, compatible with t-channel unitarity.

Recall that unitarity screening of GW ("low mass") diffraction is carried out explicitly by eikonalization, while the screening of non GW ("high mass") diffraction is carried out by the survival probability (to be discussed).

The figure shows the  $IP$  Green function. Multi  $IP$  interactions are summed differently in the various  $IP$  models. Note the analogy with QED:

- a) Enhanced diagrams, present the renormalization of the propagator.
- b) Semi enhanced diagrams, present the  $pIPp$  vertex renormalization.



## SURVIVAL PROBABILITY

The experimental signature of a  $\mathbb{P}$  exchanged reaction is a large rapidity gap (LRG), devoid of hadrons in the  $\eta - \phi$  Lego plot,  $\eta = -\ln(\tan\frac{\theta}{2})$ .

$S^2$ , the LRG survival probability, is a unitarity induced suppression factor of non GW diffraction, soft or hard:  $S^2 = \sigma_{diff}^{screened} / \sigma_{diff}^{nonscreened}$ .

It is the probability that the LRG signature will not be filled by debris (partons and/or hadrons) originating from either the s-channel re-scatterings of the spectator partons, or by the t-channel multi  $\mathbb{P}$  interactions.

Denote the gap survival factor initiated by s-channel eikonalization  $S_{eik}^2$ , and the one initiated by t-channel multi  $\mathbb{P}$  interactions,  $S_{m\mathbb{P}}^2$ .

The incoming projectiles are summed over (i,k).

$S^2$  is obtained from a convolution of  $S_{eik}^2$  and  $S_{m\mathbb{P}}^2$ .

A simpler, reasonable approximation, is  $S^2 = S_{eik}^2 \cdot S_{m\mathbb{P}}^2$ .

## INCORPORATING GOOD-WALKER AND MUELLER DIFFRACTIONS

Both the experimental and theoretical studies of soft diffraction are hindered by conflicting definitions of signatures and bounds.

In our context, I wish to discuss the relationship between GW and non GW diffraction versus Mueller's low and high diffractive mass.

Kaidalov, at the time, equated (without a proof) Mueller's low diffractive mass with GW diffraction, and high diffractive mass with non GW diffraction.

The problem is how do we define the bounds of these diffractive mass domains.

Following Kaidalov, GW low mass upper bound and Mueller's high mass lower bound, which is 4-5 GeV, coincide.

i.e. there is no overlap of low and high mass diffraction.

This point of view is shared by KMR, Ostapchenko and Poghosyan.

I find this assumption problematic, as it has no procedure which secures a smooth behaviour of the diffractive mass through this transition.

In the GLM model the GW diffractive mass is not defined. We presume (also without a proof) that GW and non GW (high mass) diffraction have the same upper bound, commonly taken to be 0.05s.

As we saw, The main difference between the 2 diffractive modes is that GW is suppressed by eikonal screenings, while non GW is suppressed by the survival probability which has an s-channel eikonal component initiated by the re-scattering of the initial projectiles and a t-channel screening induced by the multi  $\mathbb{P}$  interactions.

In GLM most of the diffraction is GW, while in KMR it is non GW high mass. Originally, GLM did not define a diffractive mass distribution. This has been amended in our recent paper, where we consider the Pomeron as a partonic probe. In this model:

$\mathbb{P}$ -q interactions contribute to GW mass distribution.

$\mathbb{P}$ -g interactions contribute to non GW, the high mass distribution.

## THE PARTONIC POMERON

Current  $\mathbb{P}$  models differ in details, but have in common a relatively large adjusted input  $\Delta_{\mathbb{P}}$  and a diminishing  $\alpha'_{\mathbb{P}}$ .

Recall that, traditionally,  $\Delta_{\mathbb{P}}$  determines the energy dependence of the total, elastic and diffractive cross sections while  $\alpha'_{\mathbb{P}}$  determines the forward slopes. This picture is modified in updated  $\mathbb{P}$  models in which s and t unitarity screenings induce a much smaller  $\mathbb{P}$  intercept at  $t=0$ , denoted  $\Delta_{\mathbb{P}}^{eff}$ , which gets smaller with energy. The exceedingly small fitted  $\alpha'_{\mathbb{P}}$  implies a partonic description of the  $\mathbb{P}$  which leads to a pQCD interpretation.

Gribov's partonic Regge theory provides the microscopic sub structure of the  $\mathbb{P}$  where the slope of the  $\mathbb{P}$  trajectory is related to the mean transverse momentum of the partonic dipoles constructing the Pomeron.

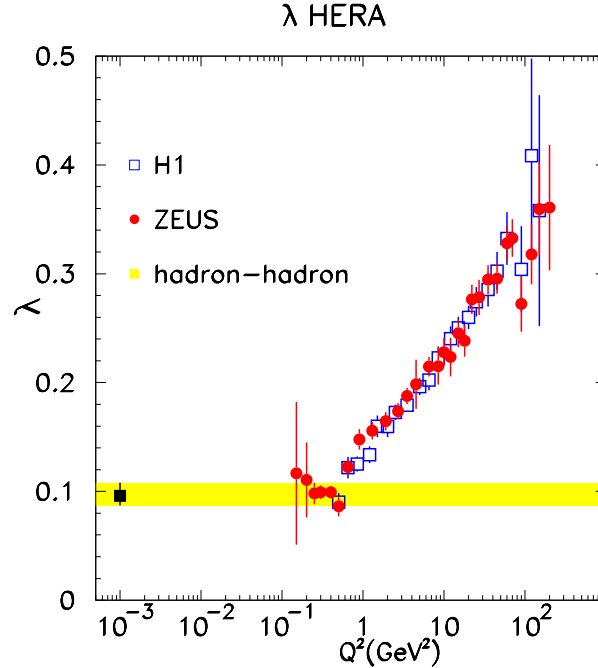
$$\alpha'_{\mathbb{P}} \propto 1 / \langle p_t \rangle^2, \quad \text{accordingly:} \quad \alpha_S \propto \pi / \ln \left( \langle p_t^2 \rangle / \Lambda_{QCD}^2 \right) \ll 1.$$

We obtain a  $\mathbb{P}$  with hardness changing continuously from hard (BFKL like) to soft (Regge like). This is a non trivial relation as the soft  $\mathbb{P}$  is a simple moving pole in J-plane, while, the BFKL hard  $\mathbb{P}$  is a branch cut, approximated, though, as a simple pole with  $\Delta_{\mathbb{P}} = 0.2 - 0.3$ ,  $\alpha'_{\mathbb{P}} \simeq 0$ .

GLM and KMR models are rooted in Gribov's partonic  $\mathbb{P}$  theory with a hard pQCD  $\mathbb{P}$  input. It is softened by unitarity screening (GLM), or the decrease of its partons' transverse momentum (KMR). The two definitions are correlated.

GLM and KMR have a bound of validity, at 60(GLM) and 100(KMR) TeV, implied by their approximations. Consequently, as attractive as updated  $\mathbb{P}$  models are, we can not utilize them above 100 TeV.

To this end, the only relevant models are single channeled, most of which have a logarithmic parametrization input. As noted, the main deficiency of these models is that they ignore the diffractive channels and their handling of unitarity screening is partial at best.



## DIS: FROM SOFT TO HARD

The single  $\mathbb{P}$  picture suggested by the updated  $\mathbb{P}$  models implies a smooth transition from the input hard  $\mathbb{P}$  to a soft  $\mathbb{P}$ . This picture is supported by the the HERA dependence of  $\lambda = \Delta_{\mathbb{P}}$  on  $Q^2$  shown in the figure above.

Note though, that a smooth transition from a soft to hard  $\mathbb{P}$  can be reproduced also by a 2  $\mathbb{P}$ s (**soft and hard**) model such as Ostapchenco's.

## UNITARITY SATURATION

As we saw, unitarity saturation is coupled to 3 experimental signatures:

$$\frac{\sigma_{inel}}{\sigma_{tot}} = \frac{\sigma_{el}}{\sigma_{tot}} = 0.5, \quad \frac{\sigma_{tot}}{B_{el}} = 9\pi, \quad \sigma_{diff} = 0.$$

Following is p-p TeV-scale data relevant to the assessment of saturation:

**CDF(1.8 TeV):**  $\sigma_{tot} = 80.03 \pm 2.24mb$ ,  $\sigma_{el} = 19.70 \pm 0.85mb$ ,  $B_{el} = 16.98 \pm 0.25GeV^{-2}$ .

**TOTEM(7 TeV):**  $\sigma_{tot} = 98.3 \pm 0.2(stat) \pm 2.8(sys)mb$ ,  $\sigma_{el} = 24.8 \pm 0.2(stat) \pm 2.8(sys)mb$ ,  
 $B_{el} = 20.1 \pm 0.2(stat) \pm 0.3(sys)GeV^{-2}$ .

**AUGER(57 TeV):**  $\sigma_{tot} = 133 \pm 13(stat) \pm_{20}^{17}sys \pm 16(Glauber)mb$ ,  
 $\sigma_{inel} = 92 \pm 7(stat) \pm_{11}^9(sys) \pm 16(Glauber)mb$ .

Note that **AUGER** margin of error of  $\sigma_{inel}$  and  $\sigma_{tot}$  output is 20%!

Consequently:  $\sigma_{inel}/\sigma_{tot} = 0.754(\text{CDF})$ ,  $0.748(\text{TOTEM})$ ,  $0.692(\text{AUGER})$ .

The numbers above suggest a very slow approach toward saturation, well above the TeV-scale. Consequently, the study of p-p saturation depends on information above the TeV-scale.

There are 2 sources from which we may obtain the desired information:

- Cosmic Rays data. Recall that p-p cross sections obtained from p-Air data have relatively large margin of error. AUGER p-p cross sections are a good example.
- Since updated  $IP$  models are confined to the TeV-scale, p-p cross sections at higher energies can be calculated only in single channeled models, the deficiencies of which have been specified before.

Out of quite a few single channeled models, I shall quote Block and Halzen, which reproduces well the inelastic and total cross sections at the TeV-scale. The BH model can be applied at exceedingly high energies.

The prediction of BH at the Planck-scale ( $1.22 \cdot 10^{16} TeV$ ) is:

$$\sigma_{inel}/\sigma_{tot} = 1131mb/2067mb = 0.547.$$

It indicates that saturation will be attained, if at all, at non realistic energies.



The predicted vanishing of the diffractive cross sections at saturation implies that  $\sigma_{sd}$ , which up to the TEVATRON grows slowly with energy, will eventually start to reduce.

This may serve as an early signature that saturation is being approached. Specifically, the preliminary TOTEM measurement of

$$\sigma_{sd} = 6.5 \pm 1.3 mb$$

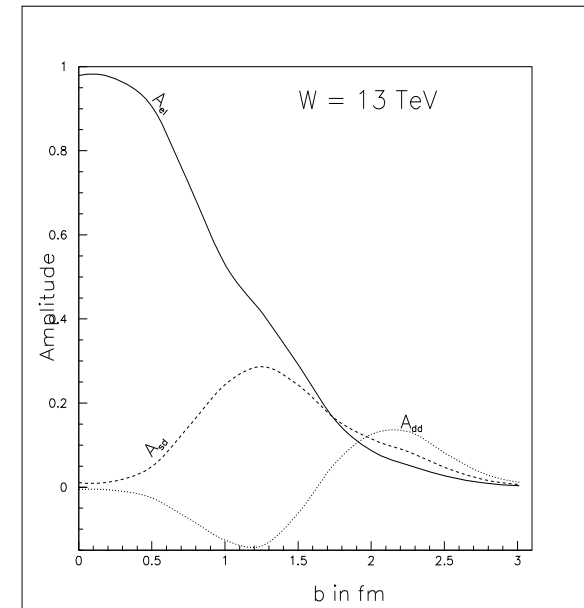
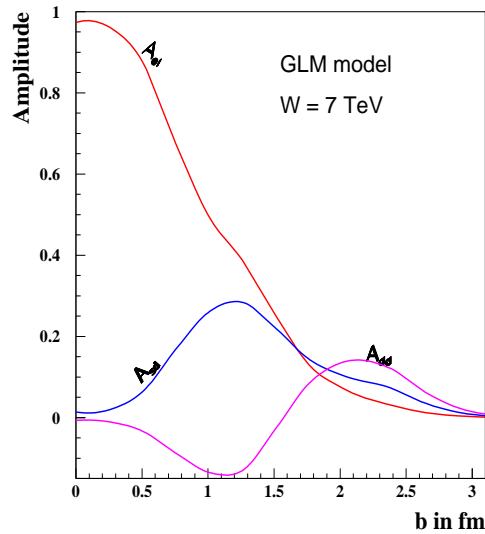
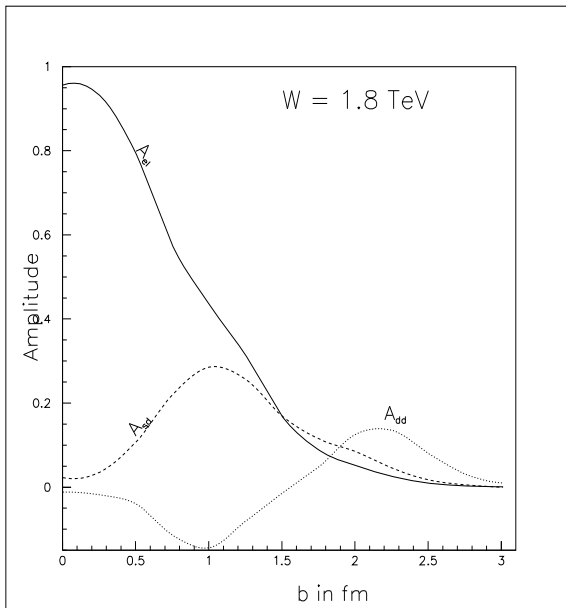
$$3.4 < M_{sd} < 1100 GeV$$

$$2.4 \cdot 10^{-7} < \xi < 0.025$$

suggests a radical change in the energy dependence of  $\sigma_{sd}$ , which is considerably smaller than its value at CDF.

$$\sigma_{sd}/\sigma_{inel} = 0.151(\text{CDF}), 0.088(\text{TOTEM}).$$

This feature, if correct, is, presently, particular to diffraction. It suggests a much faster approach toward unitarity saturation than suggested by  $\frac{\sigma_{inel}}{\sigma_{tot}}$ .



TOTEM diffractive data is very preliminary. Regardless, the compatibility between the information derived from different channels of soft scattering deserves a very careful study!

The figures above show the GLM elastic, SD and DD b-amplitudes at 1.8, 7 and 14 TeV. The difference between our output and competing models is not dramatic. **The GLM SD cross sections (in mb) are:**

$$\sigma_{sd}(W) = \sigma_{sd}^{GW} + \sigma_{sd}^{nonGW} == 8.2 + 2.07(1.8), 10.7 + 4.18(7), 11.5 + 5.81(14).$$

Recall that, EL, SD and DD cross section values are obtained from a  $b^2$  integration of the corresponding amplitude square. The growth of  $\sigma_{sd}$ , as a function of  $W$ , is mainly a consequence of  $a_{sd}(s, b)$  slow movement toward higher  $b$  values. The net result is a continuation of SD moderate increase with energy. **As a result, we do not expect a suppression of  $\sigma_{sd}$  at an energy as low as 7 TeV.** The mechanism I have just described, is straight forward. An explanation of an early reduction of the diffractive channels at relatively low energies, will require, thus, **a fundamental change in our understanding of soft scattering at the TeV-scale.**